2024 Tenth Indian Control Conference (ICC)
9 - 11 December, 2024
IISER Bhopal, India

Real-Time Implementation of a Novel LMI-Based Sliding Mode Control for Underactuated Systems in the Inertia Pendulum*

Felipe Beltrán[1], David Vázquez[1], Adolfo Soto-Cota[1], and Miguel Bernal[1]

Abstract— **This paper improves a recently appeared sliding mode control methodology for underactuated systems by translating some of its design conditions into numerically testable linear matrix inequalities, which can be solved in polynomial time via commercially available software. In this way, the original methodology which is based on the cascade normal form as well as a set of error variables that define the sliding surface, earns systematicness and flexibility as many other performance specifications can be added. The advantages of the proposal are put at test in a real-time implementation for the inertia pendulum.**

I. Introduction

Thanks to its ability to achieve finite-time convergence to a reduced-order system and, hereby, reach insensitivity to matched disturbances, standard first-order sliding mode control is one of the most popular robust control techniques [1]. First originated in the Soviet Union as the result of using discontinuous signals for control purposes [2], a number of first-order methodologies can be found in the literature, e.g., the unit vector approach [3], eigenstructure assignment [4], and continuous approximations [5]. Most of these methodologies have been successfully used in a broad number of applications [6] such as power converters [7], active suspension [8], alignment of RNA structures [9], electromechanical systems [10], rehabilitation robots [11], and control of unmanned helicopters [12], among others.

Despite its advantages, standard first-order sliding mode control usually requires the system to be put in a regular form which decouples matched and unmatched terms; moreover, it requires the input to match the dimension of the sliding surface. These characteristics usually deter designers from applying sliding mode control methodologies to underactuated systems, i.e., systems which have fewer actuators than degrees of freedom. In [13] the authors proposed a sliding mode control methodology to stabilize a class of underactuated systems, provided they are in a cascade normal form [14]. The authors prove that most mechanical systems whose mathematical model can be put in an Euler-Lagrange set of equations are amenable to the referred cascade normal form via a partial feedback linearizing controller [15] and a series of diffeomorphisms [16], e.g., the acrobot [17], the pendubot [18], the Furuta pendulum [19], the inertia wheel pendulum [20], and the inverted pendulum on a cart [21].

*This work has been supported via CONAHCYT scholarship 821527 and posdoc funding for CVU 713931 as well as the project ITSON PROFAPI CA 2024-0008.

[1]The authors are with the Dept. of Electrical and Electronics Engineering of the Sonora Institute of Technology, 5 de Febrero 818 Sur, Obregon City, Mexico, 85000, miguel.bernal@itson.edu.mx

In this work, some parts of the methodology in [13] are translated into conditions in the form of linear matrix inequalities (LMIs) [22], which can be solved in polynomial time by means of efficient algorithms already implemented in commercially available software [23]. Formulating control design proposals as sets of LMIs has become increasingly popular among control scientists due to the fact that LMIs provide a systematic framework for numerically solve otherwise complex problems [24]; when combined with the direct Lyapunov method and convex modelling of expressions, they allow for genuine nonlinear control methodologies to be implemented [25]. In the framework of sliding modes, several examples of such employment of LMIs can be found, e.g., for sliding mode controllers [26], sliding mode observers [27], sliding mode output feedback [28], etc.

The LMI additions in this proposal to the methodology in [13] are put at test in the sliding mode control of the inertia wheel pendulum, both in simulation and real-time implementation on the Mechatronics Kit by Quanser [29], which is a configurable electromechanical setup which includes a digital signal processing unit, a power module, and a MATLAB interface. The results confirm that the proposed methodology works adequately while avoiding manually tuning parameters, thanks to the LMI improvement.

This paper is organized as follows: in section II the methodology in [13] for underactuated systems is briefly presented along with a description of the inertia wheel pendulum and a short introduction to LMIs; section III develops the main results in this paper, namely, the LMI substitution of key parts of the methodology in [13] as well as its application to the inertia wheel plant; simulation and real-time results are presented in section IV, and, finally, conclusions are offered in section V.

II. Preliminaries

This section is divided in three parts: the first one is a brief description of the sliding mode control methodology in [13] which is central to our contribution; the second one describes the underactuated plant under consideration, i.e., the inertia wheel pendulum by Quanser [29]; the third one is a short introduction to the LMI framework.

A. The cascade normal form

Consider the following Euler-Lagrange form of an underactuated system with only two scalar joint variables q_1 and q_2, with $q = [q_1\ q_2]$ being the position vector, $m_{ij}(q)$, $i, j \in \{1, 2\}$ being the scalar elements of the inertia matrix, $h_i(q, \dot{q})$, $i \in \{1, 2\}$, being the scalar terms of a vector

grouping Coriolis, gravity, and friction entries, and τ being the only (scalar) actuator:

$$m_{11}(q)\ddot{q}_1 + m_{12}(q)\ddot{q}_2 + h_1(q,\dot{q}) = \tau, \quad (1)$$
$$m_{21}(q)\ddot{q}_1 + m_{22}(q)\ddot{q}_2 + h_2(q,\dot{q}) = 0. \quad (2)$$

Switching equations, this form is equivalent to [13, Equation (1)]; it is also equivalent to the case A2) in [14, Equation (2)].

In [13] it is claimed that a system of the form (1)-(2) can be put in a state-space representation of the form

$$\begin{aligned}\dot{x}_1 &= x_2 + d_1,\\ \dot{x}_2 &= f_1(x_1,x_2,x_3,x_4) + d_2,\\ \dot{x}_3 &= x_4,\\ \dot{x}_4 &= f_2(x_1,x_2,x_3,x_4) + b(x_1,x_2,x_3,x_4)u + d_3,\end{aligned} \quad (3)$$

where $x_i \in \mathbb{R}$, $i \in \{1,2,3,4\}$, are the states, $u \in \mathbb{R}$ is a virtual input, f_1, $f_2 : \mathbb{R}^4 \mapsto \mathbb{R}$, $b : \mathbb{R}^4 \mapsto \mathbb{R}$ are possibly nonlinear sufficiently smooth mappings with b invertible in a region of interest, and $d_i \in \mathbb{R}$, $i \in \{1,2,3\}$, are possibly unknown but bounded signals which may depend on states, inputs, or exogenous variables. To explain this transformation without providing details, [13] refers to [14] which, in turn, refers to the non-collocated feedback in [15]. Since these details are relevant to our contribution, they are described in the sequel.

The non-collocated feedback in [15] is a control input of the form

$$\tau = \alpha(q)u + \beta(q,\dot{q}), \quad (4)$$

where $u \in \mathbb{R}$ is a virtual input, and $\alpha(q)$ and $\beta(q,\dot{q})$ are obtained as follows:

1) Solve $\ddot{q}_1$ from (2), i.e., $\ddot{q}_1 = -m_{21}^{-1}(q)(m_{22}(q)\ddot{q}_2 + h_2(q,\dot{q}))$, and substitute it in (1), i.e., $m_{11}(q)(-m_{21}^{-1}(q)(m_{22}(q)\ddot{q}_2 + h_2(q,\dot{q}))) + m_{12}(q)\ddot{q}_2 + h_1(q,\dot{q}) = \tau$.
2) Define $\alpha(q)$ as those terms multiplying $\ddot{q}_2$ and $\beta(q,\dot{q})$ as the remaining terms on the left side, i.e., the development (omitting arguments):

$$\begin{aligned}&m_{11}\left(-m_{21}^{-1}\left(m_{22}\ddot{q}_2 + h_2\right)\right) + m_{12}\ddot{q}_2 + h_1\\ &= -m_{11}m_{21}^{-1}m_{22}\ddot{q}_2 - m_{11}m_{21}^{-1}h_2 + m_{12}\ddot{q}_2 + h_1\\ &= (m_{12} - m_{11}m_{21}^{-1}m_{22})\ddot{q}_2 + h_1 - m_{11}m_{21}^{-1}h_2 = \tau,\end{aligned}$$

allows defining $\alpha(q) = m_{12}(q) - m_{11}(q)m_{21}^{-1}(q)m_{22}(q)$ and $\beta(q,\dot{q}) = h_1(q,\dot{q}) - m_{11}(q)m_{21}^{-1}(q)h_2(q,\dot{q})$.

The substitution of τ as defined in (4) in the Euler-Lagrange system (1)-(2) yields:

$$\begin{aligned}&m_{11}\ddot{q}_1 + m_{12}\ddot{q}_2 + h_1 = (m_{12} - m_{11}m_{21}^{-1}m_{22})u + h_1 - m_{11}m_{21}^{-1}\\ &m_{21}\ddot{q}_1 + m_{22}\ddot{q}_2 + h_2 = 0,\end{aligned}$$

from which $\ddot{q}_1$ and $\ddot{q}_2$ can be solved as:

$$\begin{aligned}\ddot{q}_1 &= -m_{21}^{-1}(q)h_2(q,\dot{q}) - m_{21}^{-1}(q)m_{22}(q)u,\\ \ddot{q}_2 &= u.\end{aligned}$$

Defining $p_1 = \dot{q}_1$ and $p_2 = \dot{q}_2$, the previous equations can be equivalently described by [14]:

$$\begin{aligned}\dot{q}_1 &= p_1\\ \dot{p}_1 &= f(q,p) + g(q)u\\ \dot{q}_2 &= p_2\\ \dot{p}_2 &= u\end{aligned} \quad (5)$$

where $p = [p_1\ p_2]^T$, $f(q,p)$ and $g(q)$ are given by $f(q,p) = -m_{21}^{-1}(q)h_2(q,p)$ and $g(q) = -m_{21}^{-1}(q)m_{22}(q)$.

If $m_{ij}(q) = m_{ij}(q_2)$, $i,j \in \{1,2\}$, $m_{21}(q_2) \neq 0$, [14] proved that the change of coordinates

$$z = \begin{bmatrix} z_1\\ z_2\\ \xi_1\\ \xi_2\end{bmatrix} = T(q,p) = \begin{bmatrix} q_1 + \gamma(q_2)\\ m_{21}(q_2)p_1 + m_{22}(q_2)p_2\\ q_2\\ p_2\end{bmatrix} \quad (6)$$

puts the system into a nontriangular quadratic normal form:

$$\begin{aligned}\dot{z}_1 &= m_{21}^{-1}(\xi_1)z_2\\ \dot{z}_2 &= \left(\frac{\partial m_{21}}{\partial q_2}p_2\right)p_1 - h_2(q,p) + \left(\frac{\partial m_{22}}{\partial q_2}p_2\right)p_2\Big|_{(q,p)=T^{-1}(z)}\\ \dot{\xi}_1 &= \xi_2\\ \dot{\xi}_2 &= u,\end{aligned}$$

with $\gamma(q_2) = \int_0^{q_2}(m_{22}(s)/m_{21}(s))ds$; this system is already in the form (3) with $x_1 = z_1$, $x_2 = z_2$, $x_3 = \xi_1$, $x_4 = \xi_2$, $d_1 = m_{21}^{-1}x_2 - x_2$, $f_1 = \dot{z}_2|_{z=x}$, $f_2 = d_2 = d_3 = 0$, $b = 1$. However, thanks to the flexibility in defining d_1, f_1, d_2, f_2, b and d_3, an infinite number of possibilities with the form (3) can arise from the very same equation above.

B. Sliding mode control for underactuated systems

This section is based on [13]; it provides a globally stabilizing control law for underactuated systems in the form (3). To this end, the terms

$$\begin{aligned}&e_1 = x_1, \quad e_3 = f_1(x_1,x_2,x_3,x_4),\\ &e_2 = x_2, \quad e_4 = \frac{\partial f_1}{\partial x_1}x_2 + \frac{\partial f_1}{\partial x_2}f_1 + \frac{\partial f_1}{\partial x_3}x_4,\\ &\bar{e}_1 = [e_1\ e_2\ e_3]^T, \quad \bar{e}_2 = [e_1\ e_2]^T,\end{aligned}$$

are defined and the following assumptions are made:

$$f_1(0,0,0,0) = 0, \quad (7)$$
$$\frac{\partial f_1}{\partial x_3} \text{ or } \frac{\partial f_1}{\partial x_4} \text{ invertible}, \quad (8)$$
$$f_1(0,0,x_3,x_4) = 0 \Rightarrow x_3, x_4 \to 0, \quad (9)$$
$$d_1 \neq 0 \Rightarrow \left\|\frac{\partial f_1}{\partial x_1}\right\|_\infty \leq \beta_1,\ \beta_1 \geq 0, \quad (10)$$
$$d_2 \neq 0 \Rightarrow \left\|\frac{\partial f_1}{\partial x_2}\right\|_\infty \leq \beta_2,\ \beta_2 \geq 0, \quad (11)$$
$$d_3 \neq 0,\ \frac{\partial f_1}{\partial x_3} \text{ invertible } \Rightarrow \left\|\frac{\partial f_1}{\partial x_3}\right\|_\infty \leq \beta_3,\ \beta_3 \geq 0, \quad (12)$$
$$d_3 \neq 0,\ \frac{\partial f_1}{\partial x_4} \text{ invertible } \Rightarrow \left\|\frac{\partial f_1}{\partial x_4}\right\|_\infty \leq \beta_4,\ \beta_4 \geq 0, \quad (13)$$

$$\frac{\partial f_1}{\partial x_3} \text{ invertible } \Rightarrow \begin{cases} \|d_1\| < \bar{d}_1\|\bar{e}_1\|_2, \\ \|d_2\| < \bar{d}_2\|\bar{e}_1\|_2, \\ \|d_3\| < \bar{d}_3 + \bar{d}_4\|\zeta(x)\|_2, \end{cases} \tag{14}$$

$$\frac{\partial f_1}{\partial x_4} \text{ invertible } \Rightarrow \begin{cases} \|d_1\| < \bar{d}_1\|\bar{e}_2\|_2, \\ \|d_2\| < \bar{d}_2\|\bar{e}_2\|_2, \\ \|d_3\| < \bar{d}_3 + \bar{d}_4\|\zeta(x)\|_2, \end{cases} \tag{15}$$

with $\bar{d}_i \geq 0$, $i \in \{1,2,3,4\}$ and $\zeta(x)$ being a known vector field.

The sliding surface as well as the corresponding control laws are defined depending on whether $\partial f_1/\partial x_3$ or $\partial f_1/\partial x_4$ is invertible.

When $\partial f_1/\partial x_3$ is invertible the sliding surface is $s = 0$ with

$$s = c_1 e_1 + c_2 e_2 + c_3 e_3 + e_4, \tag{16}$$

where $c_i > 0$ are such that

$$A_{n1} = \begin{bmatrix} 0 & 1 & 0 \\ 0 & 0 & 1 \\ -c_1 & -c_2 & -c_3 \end{bmatrix}$$

is Hurwitz and $\max\{\bar{d}_1, \bar{d}_2, \beta_1\bar{d}_1 + \beta_2\bar{d}_2\} < \lambda_{\text{left}}(-A_{n1})$ where $\lambda_{\text{left}}(\mathcal{A})$ denotes the real part of the leftmost eigenvalue of $\mathcal{A}$; the equivalent control is

$$\begin{aligned} u_{\text{eq}} = &-\left[\frac{\partial f_1}{\partial x_3} b\right]^{-1} \Bigg(c_1 x_2 + c_2 f_1 + c_3 \frac{\partial f_1}{\partial x_1} x_2 + c_3 \frac{\partial f_1}{\partial x_2} f_1 + c_3 \frac{\partial f_1}{\partial x_3} x_4 \\ &+ \frac{d}{dt}\left[\frac{\partial f_1}{\partial x_1} x_2\right] + \frac{d}{dt}\left[\frac{\partial f_1}{\partial x_2} f_1\right] + \frac{d}{dt}\left[\frac{\partial f_1}{\partial x_3}\right] x_4 + \frac{\partial f_1}{\partial x_3} f_2 \Bigg); \end{aligned} \tag{17}$$

the switching control is

$$u_{\text{sw}} = -\left[\frac{\partial f_1}{\partial x_3} b\right]^{-1} \left(M \text{sign}(s) + \lambda s\right), \tag{18}$$

where $M = \left(c_1\bar{d}_1 + c_2\bar{d}_2 + c_3\beta_1\bar{d}_1 + c_3\beta_2\bar{d}_2\right)\|\bar{e}_1\|_2 + \beta_3\left(\bar{d}_3 + \bar{d}_4\|\xi(x)\|_2\right) + \rho$, for given $\rho > 0$ and $\lambda > 0$;

When $\partial f_1/\partial x_4$ is invertible the sliding surface is $s = 0$ with

$$s = c_1 e_1 + c_2 e_2 + e_3, \tag{19}$$

where $c_i > 0$ are such that

$$A_{n2} = \begin{bmatrix} 0 & 1 \\ -c_1 & -c_2 \end{bmatrix},$$

is Hurwitz with $\max\{\bar{d}_1, \bar{d}_2\} < \lambda_{\text{left}}(-A_{n2})$; the equivalent control is

$$\begin{aligned} u_{\text{eq}} = &-\left[\frac{\partial f_1}{\partial x_4} b\right]^{-1} \Bigg(c_1 x_2 + c_2 f_1 + \frac{\partial f_1}{\partial x_1} x_2 + \frac{\partial f_1}{\partial x_2} f_1 + \\ &\frac{\partial f_1}{\partial x_3} x_4 + \frac{\partial f_1}{\partial x_4} f_2 \Bigg); \end{aligned} \tag{20}$$

the switching control is

$$u_{\text{sw}} = -\left[\frac{\partial f_1}{\partial x_4} b\right]^{-1} \left(M \text{sign}(s) + \lambda s\right), \tag{21}$$

where $M = (c_1\bar{d}_1 + c_2\bar{d}_2 + \beta_1\bar{d}_1 + \beta_2\bar{d}_2)\|\bar{e}_2\|_2 + \beta_4(\bar{d}_3 + \bar{d}_4\|\xi(x)\|_2) + \rho$, for given $\rho > 0$ and $\lambda > 0$.

The complete control law in any case is $u = u_{\text{eq}} + u_{\text{sw}}$.

III. Main Results

This section has two parts: the first one provides LMI conditions for key parts of the design methodology in [13]; the second one applies the proposal to the inertia pendulum.

A. Novel LMI design conditions for underactuated systems

Calculating the coefficients c_i for matrices A_{n1} and A_{n2} above is not systematically done in [13]; an LMI solution to this problem is provided next:

Theorem 1: If there exists matrices $X \in \mathbb{R}^{3\times3}$ and $M \in \mathbb{R}^{1\times3}$ such that the LMIs

$$X = X^T > 0, \tag{22}$$

$$AX + BM + XA^T + M^T B^T + 2\alpha X < 0, \tag{23}$$

hold with $\alpha = \max\{\bar{d}_1, \bar{d}_2, \beta_1\bar{d}_1 + \beta_2\bar{d}_2\}$,

$$A = \begin{bmatrix} 0 & 1 & 0 \\ 0 & 0 & 1 \\ 0 & 0 & 0 \end{bmatrix},\ B = \begin{bmatrix} 0 \\ 0 \\ -1 \end{bmatrix},$$

then the entries of $C = [c_1\ c_2\ c_3] = MX^{-1}$ satisfy the design conditions for c_i, $i \in \{1,2,3\}$, when $\partial f_1/\partial x_3$ is invertible and $\partial f_1/\partial x_4 = 0$.

If LMIs (22)-(23) hold then we can pre- and post-multiply LMI (23) by $P = X^{-1}$, whose existence is guaranteed by LMI (22), which yields:

$$\begin{aligned} &PA + PBMP + A^T P + PM^T B^T P + 2\alpha P \\ &= P(A + BC) + (A^T + C^T B^T)P + 2\alpha P < 0 \\ &\Rightarrow P(A + BC) + (A^T + C^T B^T)P < -2\alpha P < 0 \\ &\Leftrightarrow PA_{n1} + A_{n1}^T P < -2\alpha P < 0 \end{aligned}$$

because $C = MX^{-1} = MP$, which means $A + BC = A_{n1}$ is Hurwitz [30, Proposition 4.1]; moreover, all the eigenvalues of A_{n1} are guaranteed to lie to the left of $s = -\alpha$ in the complex plane s [30, Proposition 4.3], which means that $\alpha = \max\{\bar{d}_1, \bar{d}_2, \beta_1\bar{d}_1 + \beta_2\bar{d}_2\} < \lambda_{\text{left}}(-A_{n1})$, which concludes the proof.

Similarly, an LMI solution to the problem of determining coefficients c_i when $\partial f_1/\partial x_4$ is invertible.

Theorem 2: If there exists matrices $X \in \mathbb{R}^{2\times2}$ and $M \in \mathbb{R}^{1\times2}$ such that the LMIs

$$X = X^T > 0, \tag{24}$$

$$AX + BM + XA^T + M^T B^T + 2\alpha X < 0, \tag{25}$$

hold with $\alpha = \max\{\bar{d}_1, \bar{d}_2\}$,

$$A = \begin{bmatrix} 0 & 1 \\ 0 & 0 \end{bmatrix},\ B = \begin{bmatrix} 0 \\ -1 \end{bmatrix},$$

then the entries of $C = [c_1\ c_2] = MX^{-1}$ satisfy the design conditions for c_i, $i \in \{1,2\}$, when $\partial f_1/\partial x_4$ is invertible.

Following the same lines of proof in Theorem 1, LMIs (24)-(25) guarantee $PA_{n2} + A_{n2}^T P < -2\alpha P < 0$ with $C = MX^{-1} = MP$ and $A + BC = A_{n2}$, which means the latter is Hurwitz [30, Proposition 4.1] and its eigenvalues lie to the left of $s = -\alpha$ in the complex plane s [30, Proposition 4.3], i.e., $\alpha = \max\{\bar{d}_1, \bar{d}_2\} < \lambda_{\text{left}}(-A_{n2})$, which concludes the proof.

B. Novel LMI-based control of the inertia pendulum

An inertia wheel pendulum is a mechanical device used to simulate the motion of a simple pendulum under the influence of an attached rotating wheel, which provides a sort of disturbance in the form of additional inertia (see Fig. 1). The system consists of a rigid arm that swings around a pivot point thanks to the actuated wheel attached to the end of the arm.

The Euler-Lagrange model of the inertia wheel pendulum has the form (1)-(2) with $m_{11}(q) = a_2$, $m_{12}(q) = a_2$, $m_{21}(q) = a_1 + a_2$, $m_{22}(q) = a_2$, $h_1(q, \dot{q}) = 0$, $h_2(q, \dot{q}) = -a_3 g \sin q_1$, and system parameters $a_1 = 0.9245$, $a_2 = 0.0050$, $a_3 = 7.3173$, and $g = 9.81 m/s^2$.

Using the non-collocated feedback (4) in (1)-(2), where $\alpha(q) = a_2 - a_2^2/(a_1 + a_2)$ and $\beta(q, \dot{q}) = a_2 a_3 g \sin q_1/(a_1 + a_2)$, allows solving for $\ddot{q}_1$ and $\ddot{q}_2$ to put system (1)-(2) in the state space representation (5) with q_1, q_2, $p_1 = \dot{q}_1$, and $p_2 = \dot{q}_2$ as the states, $f(q, p) = a_3 g \sin q_1/(a_1 + a_2)$, and $g(q) = -a_2/(a_1 + a_2)$. Applying the change of coordinates (6) with $\gamma(q_2) = a_2 \xi_1/(a_1 + a_2)$ to the previous model yields

$$\begin{aligned}
\dot{z}_1 &= z_2/(a_1 + a_2) \\
\dot{z}_2 &= a_3 g \sin\left(z_1 - a_2 \xi_1/(a_1 + a_2)\right) \\
\dot{\xi}_1 &= \xi_2 \\
\dot{\xi}_2 &= u,
\end{aligned}$$

which, renaming the states in terms of x and rearranging where appropriate, can be put in the normal cascade form (3) as:

$$\begin{aligned}
\dot{x}_1 &= x_2 + \left(1/(a_1 + a_2) - 1\right) x_2 \\
\dot{x}_2 &= a_3 g \sin\left(x_1 - a_2 x_3/(a_1 + a_2)\right) \\
\dot{x}_3 &= x_4 \\
\dot{x}_4 &= u,
\end{aligned}$$

where $d_1 = \left(1/(a_1 + a_2) - 1\right) x_2$, $d_2 = d_3 = 0$, $f_1 = a_3 g \sin\left(x_1 - a_2 x_3/(a_1 + a_2)\right)$, $f_2 = 0$, y $b = 1$.

This model satisfies $f_1(0, 0, 0, 0) = 0$ (assumption (7)); $\partial f_1/\partial x_3 = a_2 a_3 g/(a_1 + a_2) \cos(x_1 - a_2 x_3/(a_1 + a_2))$ is invertible for values around the origin (assumption (8)); $f_1(0, 0, x_3, x_4) = a_3 g \sin(-a_2 x_3/(a_1 + a_2)) = 0$ implies $x_3 \to 0$ and $x_4 \to 0$ (assumption (9)); since $d_1 \neq 0$ we have $\|a_3 g \cos\left(x_1 - a_2 x_3/(a_1 + a_2)\right)\|_\infty \leq a_3 g \equiv \beta_1 \geq 0$ (assumption (10)); since $d_2 = 0$ we have $\beta_2 = 0$ (assumption (11)) and since $d_3 = 0$ we have $\beta_3 = 0$ (assumption (12)). Assumptions (13) and (15) do not apply. Assumption (14) is satisfied because $\partial f_1/\partial x_3 = a_2 a_3 g/(a_1 + a_2) \cos(x_1 - a_2 x_3/(a_1 + a_2)) \neq 0$ implies $\|d_1\| = \|1/(a_1 + a_2) - 1\| \|x_2\| < (1/(a_1 + a_2) - 1) \|\bar{e}_2\|_2$, $\|d_2\| = 0$, $\|d_3\| < \bar{d}_3 + \bar{d}_4 \|\xi(x)\|_2$, with $\bar{d}_3 = 0.0001$ and $\bar{d}_4 = 0$. Therefore, the methodology in [13] is applicable with the modification introduced in Section III-A.

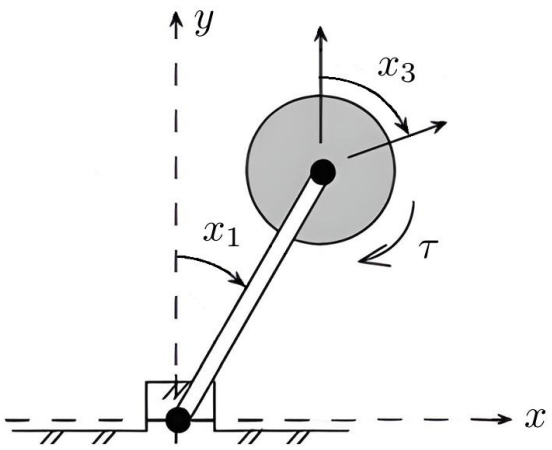


Fig. 1. The inertia wheel pendulum

Clearly, the inertia wheel pendulum where f_1 depends only on x_1 and x_3 falls in the case where $\partial f_1/\partial x_3$ is invertible and the corresponding sliding surface is defined using (16), where $e_1 = x_1$, $e_2 = x_2$, $e_3 = a_3 g \sin\left(x_1 - a_2 x_3/(a_1 + a_2)\right)$, and $e_4 = (a_3 g \cos(x_1 - a_2 x_3/(a_1 + a_2))(a_1 x_2 + a_2 x_2 - a_2 x_4))/(a_1 + a_2)$, with c_1, c_2, and c_3 determined by means of Theorem 1. In order to use LMIs (22) and (23) in the referred theorem, it is necessary to calculate $\alpha = \max\{\bar{d}_1, \bar{d}_2, \beta_1 \bar{d}_1 + \beta_2 \bar{d}_2\}$, which, in this case, yields $\alpha = \max\{0.0758, 0.0001, (71.7827)(0.0758) + (0)(0.0001)\} = 5.444$. The MATLAB LMI Toolbox has been employed to solve the LMIs; it provides the following solution:

$$X = \begin{bmatrix} 0.1520 & -0.9183 & 4.4211 \\ -0.9183 & 7.2313 & -48.2504 \\ 4.4211 & -48.2504 & 527.5291 \end{bmatrix},$$
$$M = \begin{bmatrix} -0.15 & 2.56 & 2955.35 \end{bmatrix},$$

which in turn gives $C = MX^{-1} = \begin{bmatrix} 1174.43 & 311.02 & 24.20 \end{bmatrix}$ whose entries are the sought coefficients $c_1 = 1174.43$, $c_2 = 311.02$, and $c_3 = 24.20$. As expected, the LMIs guarantee the condition without any trial-and-error procedure; indeed $\lambda_{\text{left}}(-A_{n1}) = 5.6694 > \max\{\bar{d}_1, \bar{d}_2, \beta_1 \bar{d}_1 + \beta_2 \bar{d}_2\} = 5.444$.

Thus, the sliding surface (16) is now fully defined:

$$\begin{aligned}
s =& 1174 x_1 + 311 x_2 + 1723 \sin(x_1 - 0.005379 x_3) + 71.78 x_2 \\
&\times \cos(x_1 - 0.005379 x_3) - 0.3861 x_4 \cos(x_1 - 0.005379 x_3),
\end{aligned}$$

based on which the switching control law (18) can be written:

$$\begin{aligned}
u_{\text{sw}} =& (2.6(1.2\text{e}^3 x_1 + 311 x_2 + 1.7\text{e}^3 \sin(x_1 - 5.4\text{e}^{-3} x_3) \\
&+ 72 x_2 \cos(x_1 - 5.4\text{e}^{-3} x_3) - 0.39 x_4 \cos(x_1 - 5.4\text{e}^{-3} x_3) \\
&+ \text{sign}(1.2\text{e}^3 x_1 + 311 x_2 + 1.7\text{e}^3 \sin(x_1 - 5.4\text{e}^{-3} x_3) \\
&+ 72 x_2 \cos(x_1 - 5.4\text{e}^{-3} x_3) - 0.39 x_4 \cos(x_1 - 5.4\text{e}^{-3} x_3)) \\
&\times (222(|x_1|^2 + |x_2|^2 + 5.2\text{e}^3 |\sin(x_1 - 5.4\text{e}^{-3} x_3)|^2)^{\frac{1}{2}} + 1))) \\
&/ \cos(x_1 - 5.4\text{e}^{-3} x_3),
\end{aligned}$$

where $\lambda = 1$, $\rho = 1$, and $M = 219.7(|x_1|^2 + |x_2|^2 + 5153|\sin(x_1 - 0.005379 x_3)|^2)^{1/2} + 1$ have been substituted.

The equivalent control (17) is given by:

$$
\begin{aligned}
u_{\text{eq}} =& (2.6(1.2\text{e}^3 x_2 + 2.2\text{e}^4 \sin(x_1 - 5.4\text{e}^3 x_3) + 1.7\text{e}^3 x_2 \\
& \times \cos(x_1 - 5.4\text{e}^{-3} x_3) - 9.3 x_4 \cos(x_1 - 5.4\text{e}^{-3} x_3) + 5.2\text{e}^3 \\
& \times \cos(x_1 - 5.4\text{e}^{-3} x_3) \sin(x_1 - 5.4\text{e}^{-3} x_3) + x_4(0.42 x_2 \\
& \times \sin(x_1 - 5.4\text{e}^{-3} x_3) - 2.1\text{e}^{-3} x_4 \sin(x_1 - 5.4\text{e}^{-3} x_3)) \\
& - x_2(77 x_2 \sin(x_1 - 5.4\text{e}^{-3} x_3) - .39 x_4 \sin(x_1 - 5.4\text{e}^{-3} x_3)))) \\
& / \cos(x_1 - 5.4\text{e}^{-3} x_3).
\end{aligned}
$$

The final control law is $u = u_{\text{eq}} + u_{\text{sw}}$. In the next section, results of implementing this control law both in simulation and real-time setups are shown.

IV. Implementation in the Inertia Wheel Pendulum

The results of implementing the control laws developed in the previous section are shown in the sequel. Simulations do not consider any limitation to the control magnitude $|u|$ while real-time implementations require taking into account the maximum voltage allowed for the single DC motor in the Mechatronics Kit, i.e., gains such as M and λ in the discontinuous term u_{sw} should be tuned as to hold the absolute input constraint of 23V [29]. Moreover, angular velocities are not available in real time; therefore, they should be estimated. Providers usually use 2nd-order digital filters to differentiate signals, but some researchers employ Levant's robust differentiator in combination with sliding-mode schemes [31]; to avoid complications, the provider's differentiators have been used in this work.

Fig. 2 shows the time evolution of the states when the control law $u = u_{\text{eq}} + u_{\text{sw}}$, designed in the previous section, is implemented in simulation for initial conditions $x_1(0) = 0.1$, $x_2(0) = -0.1$, $x_3(0) = 0.1$, $x_4(0) = -0.1$; it can be seen that all the states reach the desired values of 0 after a transient with noticeable overshoot; the corresponding control signal is shown in Fig. 3. It is obvious that, without saturation, this control signal is inapplicable. Fig. 4 shows the time evolution of the sliding signal $s(t)$ which reaches 0 in finite time.

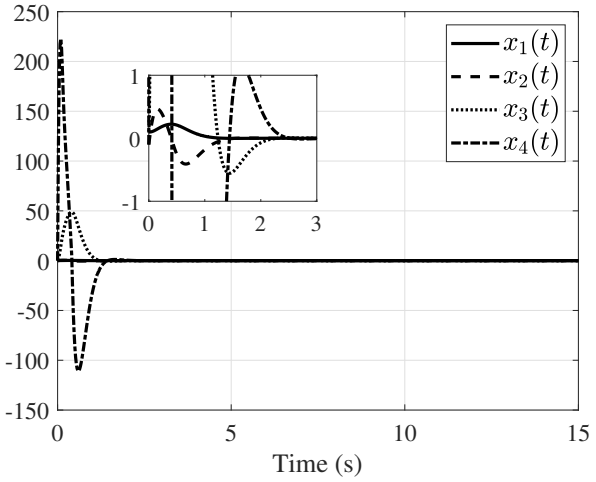


Fig. 2. Time evolution of the controlled states in simulation

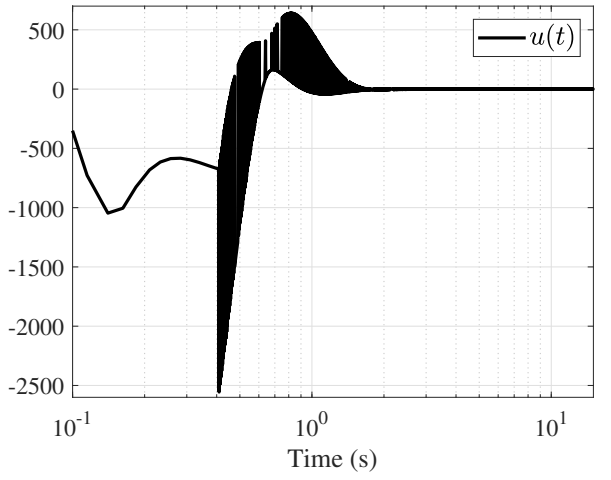


Fig. 3. Time evolution of the control signal in simulation

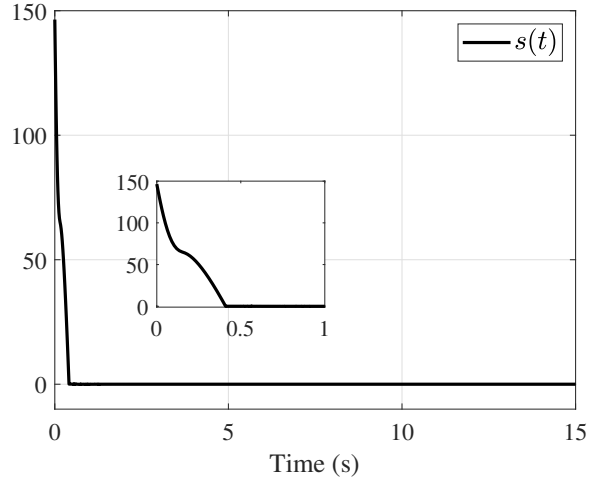


Fig. 4. Time evolution of the sliding surface

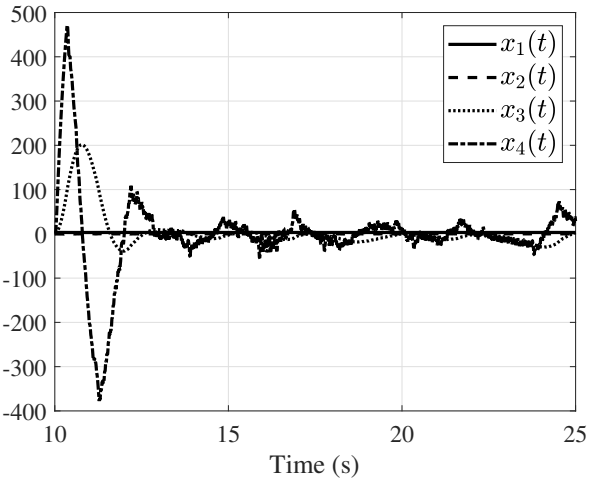


Fig. 5. Time evolution of the controlled states in real time

Fig. 5 shows the time evolution of the states when the designed control law was applied in real-time, provided a saturation was applied to the control signal shown in Fig. 6. Initial conditions are $x_1(0) = 0.2672$, $x_2(0) = 0.0252$, $x_3(0) = 0$, $x_4(0) = 0.0251$. Simultaneous stabilization of all the states in the underactuated plant takes place as expected[1].

V. Conclusions

A novel LMI-based sliding mode control methodology addressed to underactuated systems with specific Euler-Lagrange structures has been presented. It has been explicitly shown that they can be put in the cascade normal form, based on which, a set of error variables in the sliding surface can be defined. It has been proved that the coefficients of the latter can be exactly calculated via LMIs, thus improving the numerical implementability of the original technique. Simulation and real-time results in the inertia wheel pendulum have been presented.

References

[1] C. Edwards and S. Spurgeon, *Sliding mode control: theory and applications*. Padstow, UK: Taylor and Francis Ltd., UK, 1998.

[2] V. Utkin, *Sliding Modes in Control and Optimization*. Berlin: Springer, 1992, vol. 116.

[3] E. Ryan and M. Corless, "Ultimate boundedness and asymptotic stability of a class of uncertain dynamical systems via continuous and discontinuous feedback control," *IMA journal of mathematical control and information*, vol. 1, no. 3, pp. 223–242, 1984.

[4] T.-B. Lee and H.-S. Yang, "Sliding surface design by eigenstructure assignment and sliding mode control of matched uncertain systems," *Journal of Institute of Control, Robotics and Systems*, vol. 15, no. 8, pp. 812–817, 2009.

[5] T. Fliegner and M. Smith, "On the robustness of continuously approximated sliding mode schemes," *IFAC Proceedings Volumes*, vol. 31, no. 17, pp. 237–242, 1998.

[6] N. Derbel, J. Ghommam, and Q. Zhu, *Applications of sliding mode control*. Springer, 2017, vol. 79.

[7] H. Komurcugil, S. Biricik, S. Bayhan, and Z. Zhang, "Sliding mode control: Overview of its applications in power converters," *IEEE Industrial Electronics Magazine*, vol. 15, no. 1, pp. 40–49, 2020.

[1]Videos of the real-time implementations are available at `https://youtube.com/shorts/gEDMmn8UWL8?si=27b6stu0vNif62H4`.

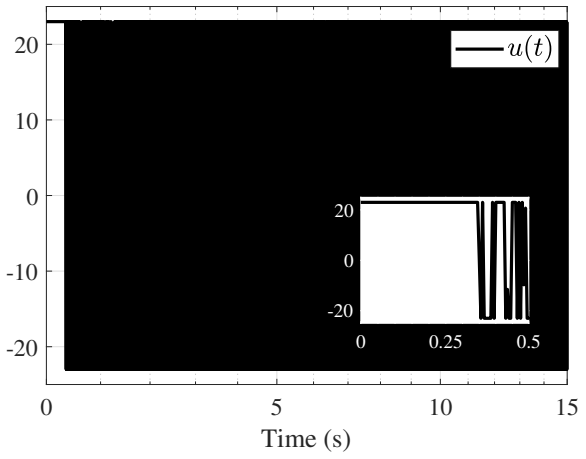


Fig. 6. Time evolution of the control signal in real time

[8] A. E. Ashari, "Sliding-mode control of active suspension systems: unit vector approach," in *Proceedings of the 2004 IEEE International Conference on Control Applications, 2004.*, vol. 1. IEEE, 2004, pp. 370–375.

[9] E. Capriotti and M. A. Marti-Renom, "Rna structure alignment by a unit-vector approach," *Bioinformatics*, vol. 24, no. 16, pp. i112–i118, 2008.

[10] V. Utkin, J. Guldner, and J. Shi, *Sliding mode control in electromechanical systems*. CRC press, 2017.

[11] S. F. Ahmed, Y. Raza, H. F. Mahdi, W. W. Muhamad, M. K. Joyo, A. Shah, and M. Koondhar, "Review on sliding mode controller and its modified types for rehabilitation robots," in *2019 IEEE 6th International Conference on Engineering Technologies and Applied Sciences (ICETAS)*. IEEE, 2019, pp. 1–8.

[12] H. Hajkarami, M. S. Ahmadi, and M. Danesh, "Unit vector approach based sliding mode control of a small-scale unmanned helicopter," in *IEEE ICCA 2010*. IEEE, 2010, pp. 28–33.

[13] R. Xu and Ü. Özgüner, "Sliding mode control of a class of underactuated systems," *Automatica*, vol. 44, no. 1, pp. 233–241, 2008.

[14] R. Olfati-Saber, "Normal forms for underactuated mechanical systems with symmetry," *IEEE Transactions on automatic control*, vol. 47, no. 2, pp. 305–308, 2002.

[15] M. W. Spong, "Energy based control of a class of underactuated mechanical systems," *IFAC Proceedings Volumes*, vol. 29, no. 1, pp. 2828–2832, 1996.

[16] R. Olfati-Saber, "Cascade normal forms for underactuated mechanical systems," in *Proceedings of the 39th IEEE Conference on Decision and Control (Cat. No. 00CH37187)*, vol. 3. IEEE, 2000, pp. 2162–2167.

[17] M. W. Spong, "The swing up control problem for the acrobot," *IEEE control systems magazine*, vol. 15, no. 1, pp. 49–55, 1995.

[18] J. Serrano-Heredia, A. G. Loukianov, and E. Bayro-Corrochano, "Sliding mode block control regulation of the pendubot," in *2011 50th IEEE Conference on Decision and Control and European Control Conference*. IEEE, 2011, pp. 8249–8254.

[19] M. Izutsu, Y. Pan, and K. Furuta, "Swing-up of furuta pendulum by nonlinear sliding mode control," *SICE Journal of Control, Measurement, and System Integration*, vol. 1, no. 1, pp. 12–17, 2008.

[20] V. M. Hernández, "A combined sliding mode-generalized pi control scheme for swinging up and balancing the inertia wheel pendulum," *Asian Journal of Control*, vol. 5, no. 4, pp. 620–625, 2003.

[21] S. Irfan, A. Mehmood, M. T. Razzaq, and J. Iqbal, "Advanced sliding mode control techniques for inverted pendulum: Modelling and simulation," *Engineering science and technology, an international journal*, vol. 21, no. 4, pp. 753–759, 2018.

[22] S. Boyd, L. E. Ghaoui, E. Feron, and V. Belakrishnan, *Linear Matrix Inequalities in System and Control Theory*. Philadelphia, USA: SIAM: Studies In Applied Mathematics, 1994, vol. 15.

[23] P. Gahinet, A. Nemirovski, A. J. Laub, and M. Chilali, *LMI Control Toolbox*. Natick, USA: Math Works, 1995.

[24] C. Scherer, *Linear Matrix Inequalities in Control Theory*. Delf, The Netherlands: Delf University, 2004.

[25] M. Bernal, A. Sala, Z. Lendek, and T. M. Guerra, *Analysis and Synthesis of Nonlinear Control Systems*. Springer, 2022.

[26] C. Edwards, "A practical method for the design of sliding mode controllers using linear matrix inequalities," *Automatica*, vol. 40, no. 10, pp. 1761–1769, 2004.

[27] C. P. Tan and C. Edwards, "An lmi approach for designing sliding mode observers," *International Journal of Control*, vol. 74, no. 16, pp. 1559–1568, 2001.

[28] C. Edwards, A. Akoachere, and S. K. Spurgeon, "Sliding-mode output feedback controller design using linear matrix inequalities," *IEEE Transactions on Automatic Control*, vol. 46, no. 1, pp. 115–119, 2001.

[29] Quanser, "Mechatronics control kit user's manual," kit manual, 2006.

[30] G. Duan and H. Yu, *LMIs in Control Systems: Analysis, Design and Applications*. CRC Press, 2013.

[31] C. Calvo, D. Vázquez, and M. Bernal, "Real-time control of underactuated systems in a mechatronics kit via a novel lmi-based sliding mode approach," in *Proceedings of the National Congress of Automatic Control*, Acapulco, Mexico, 2023.